ORIGINAL ARTICLE

WILEY MOLECULAR ECOLOGY

Late Pleistocene origin of the entire circumarctic range of the arctic-alpine plant *Kalmia procumbens*

Hajime Ikeda[1] | Pernille Bronken Eidesen[2] | Valentin Yakubov[3] |
Vyacheslav Barkalov[3] | Christian Brochmann[4] | Hiroaki Setoguchi[5]

[1]Institute of Plant Science and Resources, Okayama University, Kurashiki, Okayama, Japan

[2]The University Centre in Svalbard, Longyearbyen, Norway

[3]Federal Scientific Center of the East Asia Terrestrial Biodiversity, Far East Branch of the Russian Academy of Sciences, Vladivostok, Russia

[4]Natural History Museum, University of Oslo, Oslo, Norway

[5]Graduate School of Human and Environmental Studies, Kyoto University, Sakyo-ku, Kyoto, Japan

Correspondence
Hajime Ikeda, Institute of Plant Science and Resources, Okayama University, Kurashiki, Okayama, Japan.
Email: ike@okayama-u.ac.jp

Abstract

The circumarctic ranges of arctic-alpine plants are thought to have been established in the late Pliocene/early Pleistocene, when the modern arctic tundra was formed in response to climate cooling. Previous findings of range-wide genetic structure in arctic-alpine plants have been thought to support this hypothesis, but few studies have explicitly addressed the temporal framework of the genetic structure. Here, we estimated the demographic history of the genetic structure in the circumarctic *Kalmia procumbens* using sequences of multiple nuclear loci and examined whether its genetic structure reflects prolonged isolation throughout the Pleistocene. Both Bayesian clustering and phylogenetic analyses revealed genetic distinction between alpine and arctic regions, whereas detailed groupings were somewhat discordant between the analyses. By assuming a population grouping based on the phylogenetic analyses, which likely reflects a deeper intraspecific divergence, we conducted model-based analyses and demonstrated that the intraspecific genetic divergence in *K. procumbens* likely originated during the last glacial period. Thus, there is no need to postulate range separation throughout the Pleistocene to explain the current genetic structure in this species. This study demonstrates that range-wide genetic structure in arctic-alpine plants does not necessarily result from the late Pliocene/early Pleistocene origin of their circumarctic ranges and emphasizes the importance of a temporal framework of the current genetic structure for understanding the biogeographic history of the arctic flora.

KEYWORDS
arctic flora, IM model, phylogeography, Pleistocene, refugia

1 | INTRODUCTION

Many arctic-alpine plants have extensive distributions encompassing the entire circumarctic region as well as high mountains in North America, Europe, and East and Central Asia (Murray, 1995). During the Pleistocene, a large proportion of their current ranges were repeatedly glaciated, dramatically influencing their distributions. In his pioneering phytogeographic studies, Hultén (1937) proposed that the enormous ranges of arctic-alpine plants were established in the late Pliocene/early Pleistocene, when the modern tundra ecosystem was formed in response to climate cooling. After the initial establishment, glaciers recurrently fragmented their ranges into numerous ice-free refugia, in which large areas around the Bering Strait (Beringia) played an important role for their glacial survival and interglacial recolonization into previously glaciated areas (Abbott & Brochmann, 2003; Abbott & Comes, 2004; Hultén, 1937).

Recent phylogeographic studies of arctic-alpine plant species have revealed that their genetic variation is typically highly

wileyonlinelibrary.com/journal/mec

structured due to several major geographic barriers that facilitated range separation (17 species, Eidesen et al., 2013; *Silene acaulis*, Gussarova et al., 2015). A few studies have estimated that major lineages within arctic-alpine plants diverged prior to the middle Pleistocene (*Saxifraga oppositifolia*, Abbott, 2000; Abbott & Comes, 2004; *Vaccinium uliginosum*, Alsos, Engelskjøn, Gielly, Taberlet, & Brochmann, 2005; *Oxyria dygina*, Wang et al., 2016), consistent with Hultén's (1937) hypothesis of an early Pleistocene origin of their circumarctic ranges. However, several phylogeographic studies also suggest that some arctic-alpine plants are capable of extensive long-distance dispersal (*V. uliginosum*, Alsos et al., 2007; *Cassiope tetragona*, Eidesen, Carlsen, Molau, & Brochmann, 2007; *Saxifraga rivularis*, Westergaard, Jørgensen, Gabrielsen, Alsos, & Brochmann, 2010), even from Alaska to southern South America (*Empetrum*, Popp, Mirre, & Brochmann, 2011). In particular, the geographic structure of the genetic diversity in *C. tetragona* suggests that most of its circumarctic range was established by recent eastward recolonization from Beringia, possibly during the current interglacial period (Eidesen et al., 2007). Thus, it seems that arctic-alpine plants could have spread into their extensive ranges even during a single interglacial period. This scenario implies that range-wide genetic structure does not necessarily reflect prolonged isolation throughout the Pleistocene. Hence, assessing the temporal framework of range-wide genetic structure may improve our understanding of the historical biogeography of the arctic flora.

Kalmia procumbens (L.) Gift & Kron [*Loiseleuria procumbens* (L.) Desvaux] (Ericaceae) is an arctic-alpine plant occurring over most of the circumarctic region as well as in high mountains in the Northern Hemisphere. It is the only species of *Kalmia* that occurs outside North America (Liu, Denford, Ebinger, Packer, & Tucker, 1993; Yamazaki, 1993). According to the exclusive occurrence of the other *Kalmia* species in North America, including its sister species *Kalmia buxifolia* (Gillespie & Kron, 2013), this arctic-alpine species may have originated in North America, from where it could have spread into its current circumarctic range, however, the divergence time for *K. procumbens* is unknown. Given that it has capsules with small seeds and grows in open ridge habitats, this species may be efficiently dispersed by wind. The large-scale genetic structure in *K. procumbens* was addressed as part of a meta-study based on amplified fragment length polymorphisms (AFLPs; Eidesen et al., 2013), in which five genetic clusters were inferred: two were widespread from Beringia across the North Atlantic to northern Europe, two were restricted to northern Europe, and one was restricted to alpine areas in southern Europe (Eidesen et al., 2013). Thus, it may be hypothesized that the species experienced prolonged isolation in several refugia such as Beringia and southern and northern Europe throughout the Pleistocene. Another study revealed that central and northern Japanese populations of this species have different plastid DNA haplotypes (Ikeda, Senni, Fujii, & Setoguchi, 2009). This finding is in accordance with studies of other alpine plants showing genetic differentiation between northern and central Japan (Ikeda, Higashi, Yakubov, Barkalov, & Setoguchi, 2014; Ikeda, Senni, Fujii, & Setoguchi, 2006, 2008), where the genetic divergence was estimated to

have originated before the last glacial period (Ikeda, Fujii, & Setoguchi, 2009; Ikeda & Setoguchi, 2013; Ikeda, Higashi et al., 2014). Thus, isolated populations of *K. procumbens* may have persisted in central Japan, but their historical relationships to the remaining range remain unclear. Because *K. procumbens* is diploid (Elven, Murray, Yu, & Yurtsev, 2007; Shimizu, 1982), we can use the same approach based on sequencing of multiple nuclear genes as we used in previous studies of diploid Ericaceae species (Ikeda, Yakubov, Barkalov, & Setoguchi, 2014; Ikeda et al., 2015; Ikeda, Sakaguchi, Yakubov, Barkalov, & Setoguchi, 2016). We therefore considered *K. procumbens* to be appropriate for assessing the temporal framework underlying circumarctic genetic structure.

In this study, we (i) assess the range-wide genetic structure in *K. procumbens* based on multilocus nuclear sequence data and (ii) estimate the temporal framework of its intraspecific divergence by demographic analyses using a full-likelihood method (Hey, 2010; Hey & Nielsen, 2007). Based on these phylogeographic investigations, we aim to infer the range dynamics underlying the genetic structure in *K. procumbens* and provide further novel insights into the historical biogeography of the arctic-alpine flora.

2 | MATERIALS AND METHODS

2.1 | DNA extraction and multilocus sequencing

DNA was extracted from dried leaf materials using the DNeasy Kit (Qiagen, Hilden, Germany). In total, 73 individuals from 40 populations were included in this study (Figure 1a, Table S1). We attempted PCR amplification and subsequent direct sequencing for three phytochrome genes (Ikeda, 2012; Ikeda & Setoguchi, 2010) and 40 expressed sequence tag (EST) markers (Wei, Fu, & Arora, 2005) following the procedures in Ikeda and Setoguchi (2013). After preliminary screening, 12 EST loci exhibiting sequences with unambiguous electropherograms were chosen. Previously reported primers or newly designed ones were used for PCR amplification (Table S2). PCR products were directly sequenced from both directions using their PCR primers or internal primers that were designed based on the sequence of PCR products. The sequences between the forward and reverse primers were defined as the sequences of a given locus. Alignment was conducted using the software CLC MAIN WORKBENCH (CLC Bio, Cambridge, MA, USA). Haplotypes of each locus were determined using the software PHASE (Stephens & Donnelly, 2003; Stephens, Smith, & Donnelly, 2001), from which alignments of phased sequences of each locus were constructed using SEQPHASE (Flot, 2010). Because our procedure cannot determine sequences of loci with heterogeneous insertion or deletion polymorphisms, we treated such data as missing.

2.2 | Analyses of genetic diversity and structure

The number of segregating sites (*S*), pairwise difference (π; Tajima, 1983) and Tajima's *D* (Tajima, 1989) were calculated for each locus across samples within the groups for analyses (see Results). The
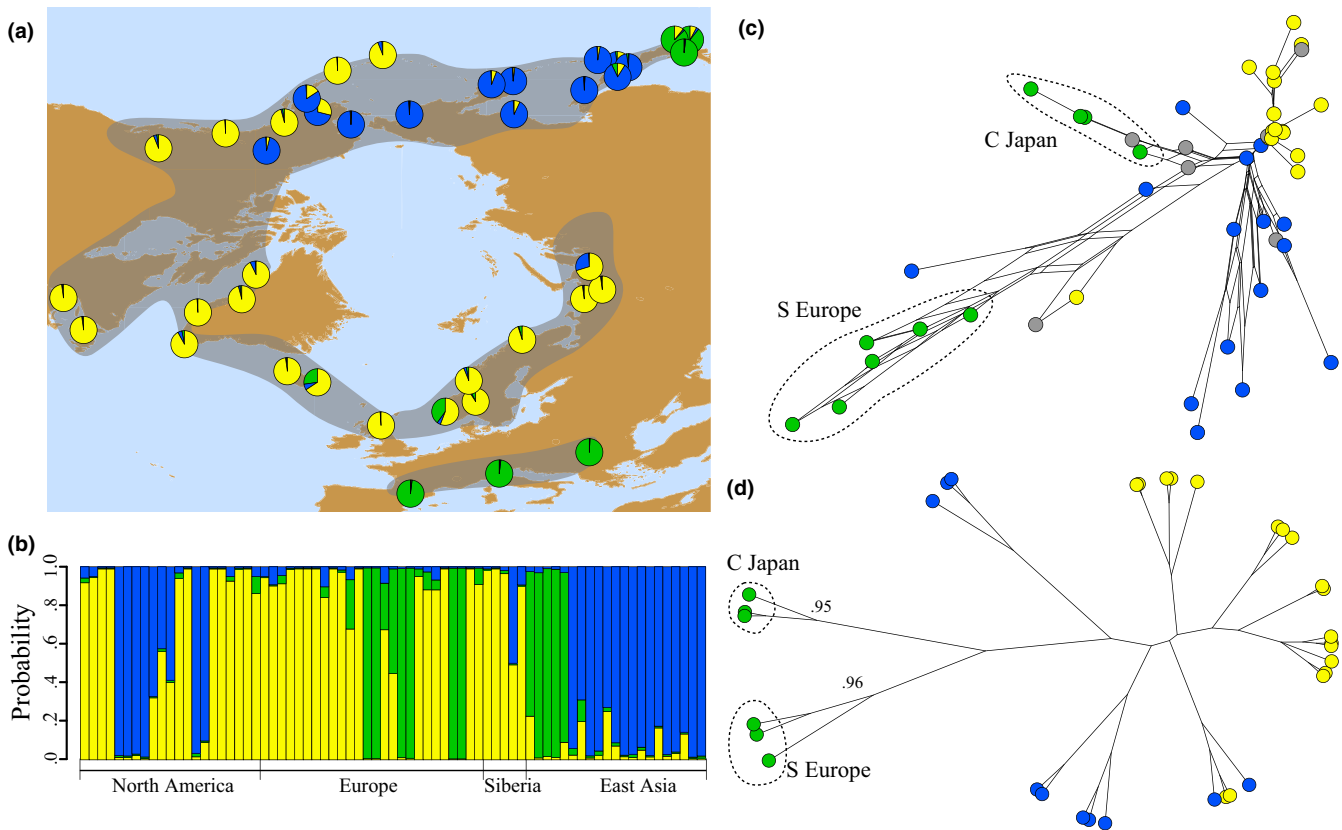
FIGURE 1 Range-wide genetic structure in *Kalmia procumbens*. (a) Map showing the geographic distribution of three clusters estimated by STRUCTURE analysis (blue, yellow and green). The probability of the clusters for each population is represented by a pie chart. The geographic range of *K. procumbens* is indicated by grey shaded areas. (b) Bar plot representing probabilities of ancestral clusters of each individual, sorted by longitude. Detailed probability data are shown in Table S1. (c) Phylogenetic relationships among individuals estimated by network analysis. Sequences of all loci (except C12) were used to resolve the phylogenetic relationships among individuals without missing data. Blue, yellow and green circles represent individuals assigned to each cluster by the STRUCTURE analysis with high probability (>0.8). Grey circles indicate the remaining individuals that were not clearly assigned to a cluster. (d) Phylogenetic relationships among populations estimated by the Bayesian analysis implemented in *BEAST. Colours correspond to the dominant clusters in each population. Nodes for highly supported groups (posterior probabilities > 0.95) are indicated by black circles

deviation from neutral expectation was examined by 1,000 coalescent simulations. All calculations and simulations of summary statistics were performed using MANVA (designed by Ramos-Onsins et al.; http://www.ub.edu/softevol/manva/).

Genetic structure was first explored by Bayesian clustering, which estimates clusters assuming Hardy–Weinberg equilibrium, using STRUCTURE version 2.3 (Falush, Stephens, & Pritchard, 2003; Pritchard, Stephens, & Donnelly, 2000). Allele data for each locus including missing data and the combination of alleles of all loci were used to estimate the probability of assigning individuals into each cluster ($K = 1$–20). By applying the default model (admixture model of ancestry and correlated allele frequency model), we performed 5.0×10^5 Markov chain Monte Carlo (MCMC) following a burn-in period of 1.0×10^5 generations. After repeating 10 independent runs, the optimal number of clusters (K) was identified based on ΔK (Evanno, Regnaut, & Goudet, 2005) and the consistency of configurations among replicate runs was evaluated using the symmetric similarity coefficient (H') calculated using CLUMPP (Jakobsson & Rosenberg, 2007).

In addition to clustering analyses based on allele data for all analysed individuals, phylogenetic relationships among both individuals and populations were resolved using sequence data of individuals having no missing data at any loci. To analyse representative individuals that covered the entire geographic range, locus C12, in which numerous individuals from central Japan have heterogeneous polymorphisms at insertions or deletions, was excluded from phylogenetic analyses (in total, 64 individuals were included). Individual relationships were estimated by neighbour-net using SPLITSTREE (Bryant & Moulton, 2004). Unphased sequences of each locus were concatenated to single matrices, where all ambiguous nucleotides (e.g., R and Y) were treated by averaging all possible resolutions under the UncorrectedP method.

Phylogenetic relationships among populations were estimated with a multispecies coalescent model using the *BEAST option in BEAST version 1.8.1 (Drummond & Rambaut, 2007; Heled & Drummond, 2010). Markov chain Monte Carlo searches were run for 1.2×10^8 iterations under possible settings of population size priors (constant population size, linear population size, constant & linear

population size), clock models (strict clock and uncorrelated lognormal relaxed clock) and substitution models (Hasegawa-Kishino-Yano [HKY] and Generalised time-reversible), from which 2.0×10^7 iterations were discarded as burn-in and every 2,000 iterations were sampled. After checking the convergence (effective sample size > 200), a replicate run was performed under the default setting (constant & linear population size prior, strict clock model and HKY substitution model) because other settings failed to converge in the setting of MCMC searches. The results of two replicate runs were combined into a single file to construct a population tree using TREEANNOTATOR version 1.8.1. To satisfy the assumption of analysis that no gene flow occurred among analysed samples, we used the same data set as used for the network analysis, except for excluding eight individuals that were not assigned to a single cluster with high probability in Bayesian clustering ($p < .80$; Table S1).

2.3 | Approximate Bayesian computation and model selection

Because phylogenetic analyses were expected to resolve deeper intraspecific divergence than clustering based on allele frequency, strongly supported phylogenetic groups (the circumarctic, southern Europe [S Europe] and central Japan [C Japan] groups; see Results) were applied to model-based analyses. Three models of possible bifurcate divergence among these groups, which included independent parameters of population size and divergence time, were assumed to estimate intraspecific divergence history (Figure 2a). To focus on testing the divergence processes among groups, we applied simple models of divergence among groups that did not incorporate gene flow between populations. The most probable model was selected by applying approximate Bayesian computation (ABC; Beaumont, Zhang, & Balding, 2002). All samples used in the BEAST analysis were assigned to each of three groups according to their geographic origin (92, 12 and 8 haploids in the circumarctic, the S Europe and the C Japan groups, respectively; Table S1), from which five categories of summary statistics (number of segregating sites, S; expected heterozygosity, H; average number of pairwise differences, π; Tajima's D; fixation index, F_{ST}) were calculated as an observed data set (in total 26, statistics; Table S3).

Under each model, 1.0×10^5 data sets with the same number of samples in each group and loci with the observed data set were generated using FASTSIMCOAL2 (Excoffier, Dupanloup, Huerta-Sánchez, Sousa, & Foll, 2013; Excoffier & Foll, 2011). Because we lack knowledge regarding these demographic parameters, large priors were applied for each parameter (population size $[N] = 1.0 \times 10^2$–1.0×10^7 haploid individuals, divergence time = 1.0×10^3–2.0×10^6 year; a log-uniform distribution was assumed for all priors). Additionally, we incorporated a mutation rate as a parameter with a prior range of 5.3–7.8×10^{-9} substitutions per site per year with a uniform distribution. This range was obtained from the substitution rate estimated in mutation accumulation lines of the model plant *Arabidopsis thaliana* (5.3–7.8×10^{-9} substitutions per site per generation; Ossowski et al., 2010). Because *A. thaliana* is an annual

herb, we applied the per-generation substitution rate as the per-year rate (i.e., 5.3–7.8×10^{-9} substitutions per site per year) to scale demographic parameters. Although we applied the per-generation substitution rate of an annual herb species as the per-year rate of the perennial shrub, the applied range was close to the synonymous substitution rates between monocots and eudicots (6.1–8.1×10^{-9} substitutions per site per year; Wolfe, Li, & Sharp, 1987). Thus, we are confident that our assumption on mutation rate provided a reasonable approximation for scaling demographic models in ABC.

Model selection was performed by a multinomial logistic regression (Beaumont, 2008) using 1.0% of the simulated data sets with the smallest Euclidean distances from the observed data set in terms of summary statistics. The power of the model selection was evaluated using a cross-validation: the summary statistics simulated under one of a given model are used as pseudo-observed data sets and classified into each model using all of the remaining simulated data sets. This procedure was performed with 100 pseudo-observed data sets from each model. Model selection was performed with the R package abc (Csilléry, François, & Blum, 2012).

2.4 | Estimating demographic parameters

The demographic parameters of the divergence model of *K. procumbens* were estimated by a full-likelihood-based model using the program IMA2 (Hey, 2010) instead of ABC. IMA2 uses genealogical data of each locus to estimate demographic parameters, whereas ABC depends on summary statistics that capture only a part of the sequence data information (Nielsen & Beaumont, 2009). Therefore, IMA2 is superior to ABC in estimating demographic parameters using sequence data in isolation-with-migration models as in the present case. We assumed a model with the most probable divergence process (Model_1; Figure 2a) and all independent parameters of IMA2 including the migration rates between all pairs of populations (population size $[\theta]$, migration rate $[m]$ between pairs of groups, and divergence time $[t]$). Parameter estimations were performed by 1.0×10^7 MCMC steps following a 500,000 generation burn-in period with 12 heated chains under the geometric increment model using all individuals originating from each group (Table S1). Three independent runs were conducted, from each of which 100,000 genealogies were saved. Prior probability densities were optimized based on several preliminary runs using a wide range of densities [$m = 0.5$ (mean of the exponential prior distribution), q (θ) = 5.0, and $t = 1.0$]. The marginal posterior distribution, maximum-likelihood estimates (MLEs) and 95% highest probability densities (95% HPDs) of each parameter were obtained using all saved genealogies. The demographic parameters were scaled by two substitution rates (5.3×10^{-9} and 7.8×10^{-9} substitutions per site per year) following the range applied in the model selection by ABC (see above), by which we estimated the range of scaled divergence time.

IMA2 assumed a constant population size to estimate demographic parameters, whereas postglacial range expansion was inferred for the circumarctic group. To evaluate the influence of range expansion on the temporal framework of intraspecific
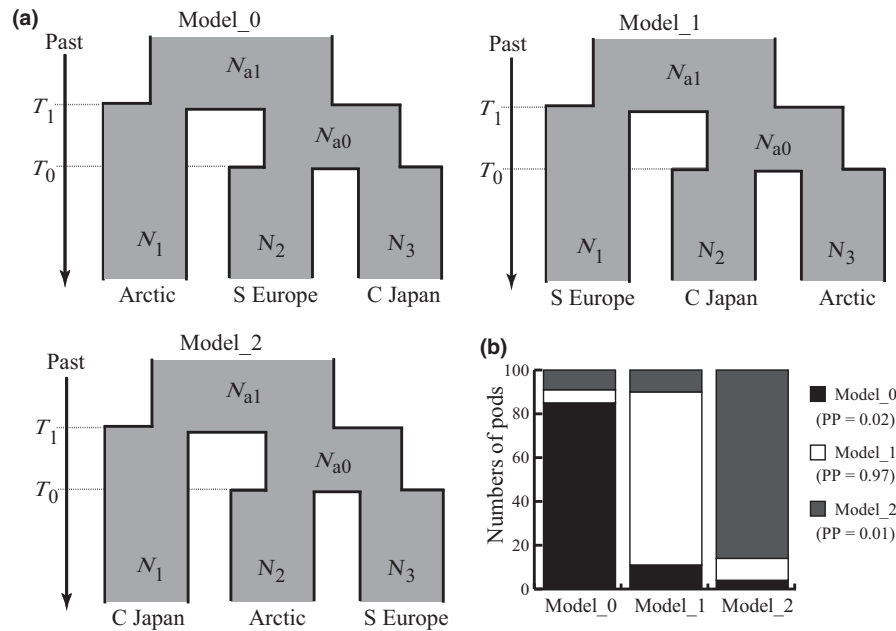
FIGURE 2 Assumed models of divergence among three geographic groups based on phylogenetic relationships of *Kalmia procumbens* and results of model selection. (a) Schematic diagrams of each model. N_X (X = 1, 2, 3) and N_{aY} (Y = 0, 1) indicate independent parameters of population sizes of extant and ancestral populations. T_Y represents the divergence time of a pair of groups. "Arctic" indicates the circumarctic group. (b) Cross-validation results for the model comparison in approximate Bayesian computation analysis. For the bar plots of each model, the sections are distinguished by different colours representing the proportions of the pseudo-observed data sets (pods), supporting a given model with highest posterior model probability. The relative posterior probability of each model is shown in parentheses

divergence, we applied ABC with a model incorporating exponential population growth into the circumarctic group following its divergence in the most probable model (Model_1). Under this model as well as Model_1, we simulated 1.0×10^5 data sets using the same settings as in the above procedure, from which 1.0×10^4 simulated data sets (0.1%) closest to the observed data were used to estimate the 95% HPDs of the initial divergence time among the groups (T_1 in Figure 2a). A local linear ridge regression was performed in parameter estimation using the R package abc (Csilléry et al., 2012).

3 | RESULTS

3.1 | Genetic diversity and structure

Twelve EST loci were sequenced, from which 5,759 bp (235–626 bp per locus; Table S3) were analysed to assess the range-wide genetic structure in *Kalmia procumbens*. According to the ΔK criteria, the optimal number of clusters obtained by Bayesian clustering was $K = 3$ (Fig. S1, Table S1), for which repeated runs exhibited a consistent configuration of individual assignments into each cluster ($H' = 1.00$). One of the clusters occurred across Beringia and extended into northern Japan, with its eastern range limit in Siberia (Figure 1a: blue). Another cluster spanned from western North America across the Atlantic into northern Europe, including western Siberia (Figure 1a: yellow). The third cluster showed a highly disjunct distribution, occurring in central Japan and southern Europe, with partial occurrence in northern Europe (Figure 1a: green). Ten

individuals were not assigned to a single cluster with high probability ($p < .80$) and exhibited genetic admixture between two clusters (e.g., three in northern Europe exhibited an admixture between yellow and green clusters; Figure 1b, Table S1).

Network analysis confirmed genetic similarity among individuals assigned to the blue and yellow clusters (Figure 1c). Individuals assigned to the green cluster formed two distantly related groups corresponding to different geographic origins (Figure 1c, central Japan and southern Europe). The phylogenetic analyses resolved two highly supported groups of populations in southern Europe and central Japan, respectively [posterior probability (PP) > 0.95; Figure 1d]. However, the remaining populations, which were dominated by one of two widespread clusters (blue and yellow clusters), did not form any highly supported groups (Figure 1d). Given that the allele data used in Bayesian clustering more likely reflected recent population dynamics than variation in the sequences used in phylogenetic analyses, the phylogenetic analyses may be appropriate to resolve a deeper history of intraspecific divergence in the species than Bayesian clustering. Thus, we applied the two exclusive phylogenetic groups in southern Europe and central Japan to assess the temporal frameworks of intraspecific divergence. Although the remaining populations did not form a single highly supported group ($PP = 0.68$), they were pooled as a third group (hereafter, the circumarctic group). As a consequence, we assumed three geographic groups for further analyses.

As expected from the larger number of samples, the number of segregating sites was higher in the circumarctic group (in total

$S = 67$) than in the other groups ($S = 18$ and 13 in the S Europe and the C Japan groups, respectively; Table 1). Genetic diversity was lower in the C Japan group (average $\pi = 0.0006$; Table 1) than in the other groups ($\pi = 0.0010$ and 0.0012 in the circumarctic and the S Europe groups, respectively; Table 1). Tajima's D exhibited a negative tendency in the circumarctic and the C Japan groups ($D = -1.06$ and -0.91, respectively; Table 1), whereas it was positive in the S Europe group ($D = 0.41$; Table 1). Significant negative deviations in D from the neutral expectation were detected in five loci in the circumarctic group (C1, C11, C16, C20 and C27; Table 1, $p < .05$). Although such significant deviations might reflect a selective sweep and/or purifying selection, the locus-wide tendency of negative D indicates that the significant negative D is less likely to reflect evidence of selective forces on the loci than neutral demographic history such as population growth. Therefore, it is reasonable to assume that the analysed loci are appropriate to resolve intraspecific divergence history.

3.2 | Divergence history among intraspecific groups

Model_1 exhibited the highest PP among the three models ($PP = 0.97$; Figure 2b). Cross-validation showed that approximately 80% of the pseudo-observed data sets of each model were assigned to their original model and that false-positive and false-negative rates were at most approximately 10% (Figure 2b). Thus, our data had the power to distinguish among the assumed models.

Three repeated runs of IMA2 exhibited consistent values in terms of MLEs and 95% HPDs (data not shown), indicating that the estimated parameters were robust. The groups of extant populations exhibited larger population sizes than their ancestral population ($\theta_A = 0.10$, 95% HPD = 0.00–0.55; Table 2, Figure 3), of which the circumarctic group exhibited the largest ($\theta_1 = 0.74$, 95% HPD = 0.47–1.15; Table 2, Figure 3) followed by the S Europe and C Japan groups ($\theta_2 = 0.28$, 95% HPD = 0.12–0.62; $\theta_3 = 0.27$, 95% HPD = 0.06–1.63; Table 2, Figure 3). All 95% HPDs of migration rates backward in time spanned zero ($m = 0.00$) except for one case ($m_{1>2} = 0.36$, 95% HPD = 0.04–1.10; Table 2, Figure 3), which represented migration from the S Europe group to the circumarctic group. The initial divergence of the S Europe group in *K. procumbens* coincided with the last glacial period in terms of MLEs ($T_1 = 53.3$–78.6 ka, Table 2; Gibbard & Van Kolfschoten, 2004), whereas its 95% HPD spanned the last two glacial cycles (95% HPD: $T_1 = 27.1$–228.2 ka; Table 2). The C Japan group likely diverged during the last glacial period ($T_0 = 43.9$–64.8 ka, Table 2), whereas its 95% HPD included the last interglacial period (95% HPD: $T_0 = 21.7$–113.4 ka; Table 2). The temporal framework of the initial divergence of the S Europe group was compatible with the estimated ranges by ABC under either Model_1 (95% HPD: $T_1 = 31.5$–161.5 ka) or its nested model including exponential growth in the circumarctic group (95% HPD: $T_1 = 44.2$–164.3 ka). Therefore, population growth following postglacial range expansion likely did not influence the present estimation of the temporal framework.

4 | DISCUSSION

Our phylogeographic investigation revealed genetic structuring across range-wide samples of *Kalmia procumbens* (Figure 1a). Given the intraspecific groups inferred by the phylogenetic analyses (Figure 1d) and the general assumption on mutation rates, we demonstrated that the intraspecific divergence across range-wide samples of *K. procumbens* likely originated during the last glacial period

TABLE 1 Summary statistics of 12 nuclear loci within analysed geographic groups of *Kalmia procumbens*. Length of analysed loci (bp), number of haploid sequences (*n*), number of segregating sites (*S*), average number of pairwise nucleotide differences (π) and Tajima's D (D) are shown. The total number (*S*) and averages (π and D) of each group are shown in the bottom row

		The circumarctic					S Europe					C Japan				
Locus	bp	n	S	π	D	p	n	S	π	D	p	n	S	π	D	p
C1	613	124	7	0.0004	−1.83	<.05	12	3	0.0017	0.22	.37	10	1	0.0006	0.01	.58
C11	237	124	7	0.0013	−1.72	<.01	12	1	0.0022	1.38	.11	10	2	0.0023	−0.69	.64
C12	433	120	7	0.0014	−1.20	.89	12	2	0.0016	0.15	.43	4	0	0.0000	na	na
C15	580	124	4	0.0010	−0.35	.57	12	1	0.0008	1.07	.25	10	2	0.0007	−1.40	.86
C16	492	116	3	0.0001	−1.53	.01	12	2	0.0014	0.22	.39	10	1	0.0004	−1.11	.47
C17	363	124	5	0.0027	0.14	.38	12	1	0.0011	0.54	.41	10	2	0.0011	−1.40	.85
C20	561	122	4	0.0002	−1.58	.01	12	0	0.0000	na	na	10	0	0.0000	na	na
C27	596	124	9	0.0009	−1.61	.01	12	4	0.0030	1.19	.14	10	0	0.0000	na	na
C34	381	124	2	0.0008	−0.20	.48	12	1	0.0011	0.54	.38	10	0	0.0000	na	na
C36	631	118	12	0.0019	−1.20	.90	12	3	0.0008	−1.63	.94	10	3	0.0015	−0.43	.63
C47	562	124	4	0.0010	−0.47	.63	12	0	0.0000	na	na	10	1	0.0004	−1.11	.47
C58	582	120	3	0.0003	−1.19	.90	12	0	0.0000	na	na	10	1	0.0003	−1.11	.46
Summary			67	0.0010	−1.06			18	0.0012	0.41			13	0.0006	−0.91	

TABLE 2 Demographic parameters of the isolation-with-migration model among three geographic groups of *Kalmia procumbens*. The MLE and 95% highest posterior density (95% HPD) are shown for population sizes (θ) of each cluster (θ_X; X = 1, 2, 3 and 4, corresponding to the circumarctic group, the S Europe group, the C Japan group and the ancestral population of the circumarctic and the C Japan groups, respectively) and ancestral population (θ_A), migration rates (*m*) backward in time between pairs of groups and divergence times of the S Europe group (t_1) and the C Japan group (t_0). The divergence time was scaled by a range of substitution rates ($5.3-7.8 \times 10^{-9}$ substitutions per site per year). Bold italic indicates a migration rate significantly larger than zero

	IMA2	
Parameters	**MLE**	**95% HPD**
Population sizes		
θ_1	0.743	0.472–1.148
θ_2	0.287	0.117–0.618
θ_3	0.268	0.058–1.633
θ_4	0.003	0.000–4.532
θ_A	0.102	0.000–0.552
<Migration rate:m>		
$m_{1>2}$	*0.355*	0.035–1.095
$m_{2>1}$	0.005	0.000–1.165
$m_{1>3}$	0.005	0.000–0.765
$m_{3>1}$	0.005	0.000–1.095
$m_{2>3}$	0.085	0.000–1.805
$m_{3>2}$	0.105	0.000–1.315
$m_{2>4}$	0.005	0.000–1.765
$m_{4>2}$	0.005	0.000–1.535
<Divergence time: t>		
t_0	0.155	0.076–0.271
t_1	0.188	0.096–0.544
Scaled divergence time (T:kya)		
T_0	43.9–64.8	21.7–113.4
T_1	53.3–78.6	27.1–228.2

HPD, highest probability densitiel MLE, maximum-likelihood estimate.

(T_1 = 53.3–78.6 ka in MLE; Table 2). Although the previous interglacial and penultimate glacial periods could not be excluded from the timing of initial divergence (95% HPD T_1 = 27.1–228.2 ka; Table 2), the estimated temporal framework indicates that there is no need to postulate refugial isolation throughout the Pleistocene to explain the current genetic structure in this species. Instead, the genetic structure could be explained by range dynamics during the latest glacial-interglacial cycle.

4.1 | Range-wide genetic structure and phylogeographic inference

The geographic distribution of clusters estimated by Bayesian clustering (Figure 1a) reflects differences in allele frequency among populations, which may provide insight into the most recent range shifts
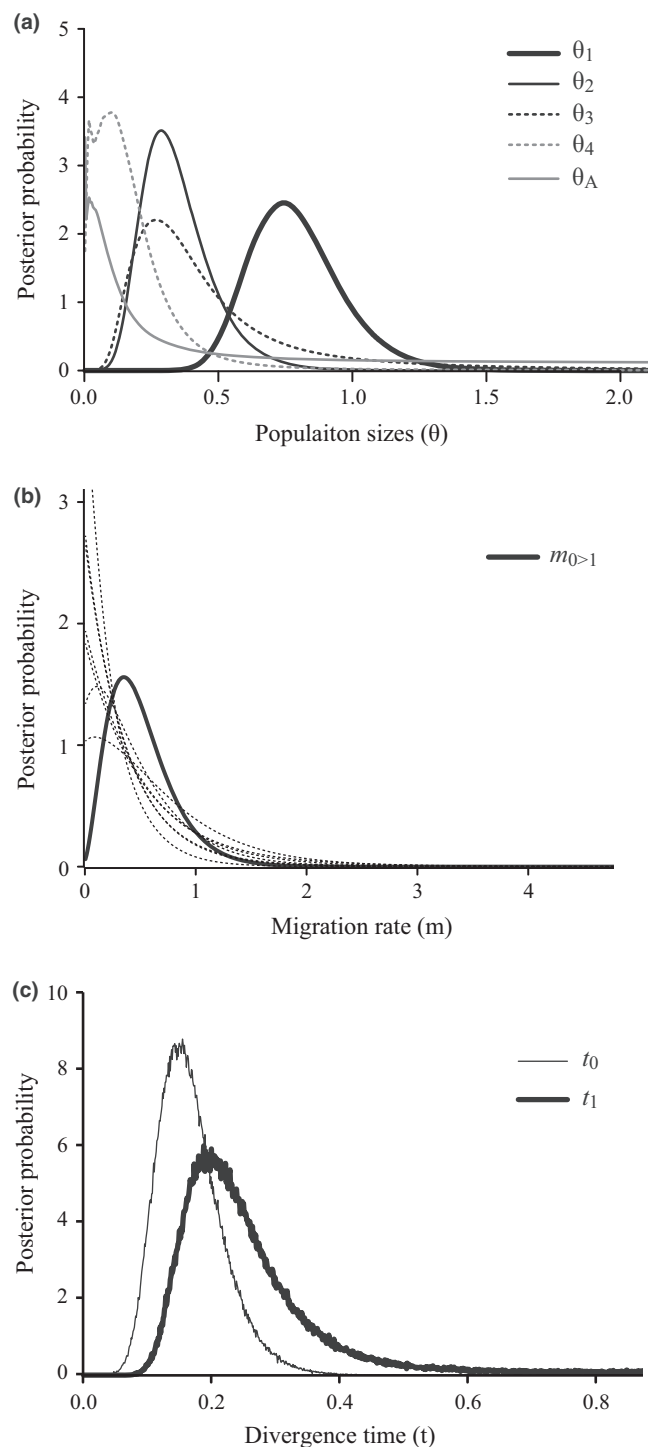

FIGURE 3 Distributions of posterior probability of demographic parameters of *Kalmia procumbens* under an isolation-with-migration model estimated using the program IMA2. (a) Population sizes of each geographic group as well as the ancestral population, (b) migration rates between pairs of groups backward in time and (c) divergence times. Migration rates are shown by dashed lines except in one significant case

of *K. procumbens*. The yellow cluster occupies areas that were mostly glaciated during the last glacial maximum. The widespread occurrence of this cluster plausibly reflects range expansion of

K. procumbens that occurred after the last glaciation. Given that this cluster was found in the eastern rather than the western part of Beringia (Figure 1a), it is most likely that eastward colonization from Beringia has resulted in the current circumarctic distribution of *K. procumbens*.

The geographic distribution of the yellow cluster corresponds to three of the five clusters estimated for *K. procumbens* using AFLP markers (Eidesen et al., 2013), whereas the previous study inferred two additional clusters in northern Europe. In the present study, a few individuals in northern Europe showed genetic admixture between the yellow and green clusters (Figure 1a, b and Table S1). Given the relict populations inferred in southern Europe, this genetic admixture may be attributed to secondary contact between individuals originating from both southern Europe and Beringia. Gene flow inferred from the S Europe group to the circumarctic group (Figure 3, Table 2) is consistent with this scenario. Thus, genetic admixture following postglacial range contact can explain the two additional clusters inferred in northern Europe based on the AFLP analysis (Eidesen et al., 2013).

The blue cluster occurs in Beringia and in northern Japan (Figure 1), which largely corresponds to the widespread AFLP cluster dominating in Beringia (no Japanese samples were included in the AFLP study of Eidesen et al., 2013). Recent phylogeographic studies have revealed genetic similarity as well as demographic closeness between northern Japan and Beringia in alpine as well as arctic-alpine plants (Hata et al., 2017; Ikeda, Higashi et al., 2014, Ikeda et al., 2016), suggesting that cold-adapted species may have spread widely in northern East Asia. Thus, the present distribution of the blue cluster probably reflects an extensive distribution of *K. procumbens* across northern East Asia and Beringia during the last glacial period, which is consistent with the history of little glaciation in this region (Frenzel et al., 1992). Notably, we found that one individual from the eastern range limit in Siberia was equally assigned to the blue and yellow clusters (Figure 1a,b and Table S1), suggesting that *K. procumbens* may have dispersed further westward from Beringia. Although more samples from this region are necessary to test this scenario rigorously, the AFLP cluster corresponding to the blue cluster has a similarly disjunct distribution (Eidesen et al., 2013), supporting this notion.

Although phylogenetic analyses did not support distinct groups of the yellow and blue clusters estimated by the Bayesian clustering (Figure 1c,d), the estimated temporal framework implies that their divergence likely did not predate the last glacial period. Because range expansion from refugia causes a reduction in genetic diversity (Hewitt, 1996) as well as changes in allele frequencies via founder effects, it is reasonable to postulate that postglacial range expansion from Beringia was involved in the divergence between the blue and yellow clusters. This hypothesis is corroborated by their distribution patterns; the blue cluster mainly occurs in continuously unglaciated areas, whereas the yellow cluster mainly occurs in previously glaciated areas.

In contrast to the two widespread clusters, the green cluster showed a disjunct occurrence in high mountains at lower latitudes in southern Europe and central Japan (Figure 1a). However, in our phylogenetic analyses, the southern European populations and the central Japanese ones were inferred to be distantly related to each other (Figure 1c,d). This inconsistency may have resulted from differences in resolution of genetic structure: that is, the resolution of the allele data used in our Bayesian clustering may have been too low to detect phylogenetic signals that were resolved by the sequence data used in the phylogenetic analyses. Therefore, it is reasonable to hypothesize that *K. procumbens* experienced specific histories of range dynamics in southern Europe and central Japan, as expected from the genetic uniqueness observed in previous AFLP (Eidesen et al., 2013) or cpDNA (Ikeda, Fujii, et al., 2009) studies. Furthermore, given our estimated temporal framework of intraspecific divergence in *K. procumbens*, these two disjunct groups may have diverged following range dynamics during the last glacial period. In this case, continental ice-sheets may have excluded most of its past range from Europe, resulting in refugial survival and unique genetic divergence in southern Europe. Conversely, given the little glaciation in East Asia, southward migration from refugial areas in northern East Asia may have been involved in genetic divergence in central Japan.

4.2 | Temporal framework of genetic structure

We acknowledge that there are certain limitations to our data sets and the analyses employed. Because we analysed only a few individuals per population, the genetic diversity of each population could not be properly assessed. Moreover, our analyses contained a limited number of loci compared with data obtained using next-generation sequencing (e.g., Massatti & Knowles, 2016; Sim, Hall, Jex, Hegel, & Coltman, 2016; Sun, Surget-Groba, & Gao, 2016). As a consequence, our analysis may have result in a reduced resolution of genetic variation and structure. Nevertheless, the range-wide genetic structure inferred in this study is largely consistent with a previous AFLP-based study (Eidesen et al., 2013), which implies that our study revealed a representative genetic structure and intraspecific divergence history. In addition to the limitations regarding the genetic structure, it should also be noted that the population grouping we used for estimating temporal framework may not necessarily represent the only possible assignment of populations in this species. Although alternative groupings likely influenced parameter estimation, the present grouping based on phylogenetic analyses may represent a deeper genetic divergence in *K. procumbens* and is unlikely to have underestimated the temporal framework. While these limitations have little influence on our inference, the present temporal framework is based on assumed mutation rates. Although reasonable mutation rates were applied for scaling divergence times, our inference is dependent on assumed rather than fossil-based rates.

With these limitations in mind, we concluded that the range-wide genetic structure in *K. procumbens* does not reflect prolonged range isolation throughout the Pleistocene. The genetic structure

observed in many arctic-alpine plants has been thought to result from prolonged isolation (Eidesen et al., 2013) and thus to support the hypothesis of a late Pliocene/early Pleistocene origin of their circumarctic ranges (Abbott, 2000; Abbott & Comes, 2004; Alsos et al., 2005; Hultén, 1937). In contrast, by explicitly estimating the temporal framework of the range-wide genetic structure, our study demonstrates that the previous conclusion may not apply to range dynamics of all arctic-alpine plants. However, this finding does not directly refute the hypothesis of a late Pliocene/early Pleistocene origin of the circumarctic range of arctic-alpine plants (Hultén, 1937). In the previous study of *Cassiope tetragona* (Eidesen et al., 2007), its current circumarctic genetic structure suggested a range expansion from Beringia after the last glaciation, whereas fossil finds from Greenland indicated its presence there as early as 2.5–2.0 Ma. Thus, our study, along with previous study, suggests that the range dynamics underlying the current genetic structure are not necessarily relevant to the initial establishment of circumarctic ranges. Accordingly, this study demonstrates that the range-wide genetic structure in arctic-alpine plants is not sufficient as evidence for their prolonged population persistence throughout the Pleistocene. Assessing the temporal framework of the current genetic structure could provide insight into the timing of range separation as well as expansion of arctic-alpine plants in the Pleistocene and improve our understanding of the historical biogeography of the arctic flora by addressing how complicated historical processes shaped current circumarctic distributions of arctic-alpine plants.

AUTHOR CONTRIBUTIONS

H.I. designed the research, collected samples, performed the experiments and the data analyses, and drafted the manuscript with the help of P.B.E. and C.B. P.B.E., V.Y., V.B., C.B. and H.S. collected samples and contributed to the writing of the manuscript.

DATA ACCESSIBILITY

DNA sequences: NCBI, LC188020-LC188882.

Alignment file of each locus and files relevant to analyses: Dryad https://doi.org/10.5061/dryad.24fb2.

ORCID

Hajime Ikeda http://orcid.org/0000-0002-3014-3585

REFERENCES

Abbott, R. J. (2000). Molecular analysis of plant migration and refugia in the Arctic. *Science*, *289*, 1343–1346.

Abbott, R. J., & Brochmann, C. (2003). History and evolution of the arctic flora: In the footsteps of Eric Hultén. *Molecular Ecology*, *12*, 299–313.

Abbott, R. J., & Comes, H. P. (2004). Evolution in the Arctic: A phylogeographic analysis of the circumarctic plant, *Saxifraga oppositifolia* (Purple saxifrage). *New Phytologist*, *161*, 211–224.

Alsos, I. G., Eidesen, P. B., Ehrich, D., Skrede, I., Westergaard, K., Jacobsen, G. H., . . . Brochmann, C. (2007). Frequent long-distance plant colonization in the changing Arctic. *Science*, *316*, 1606–1609.

Alsos, I. G., Engelskjøn, T., Gielly, L., Taberlet, P., & Brochmann, C. (2005). Impact of ice ages on circumpolar molecular diversity: Insights from an ecological key species. *Molecular Ecology*, *14*, 2739–2753.

Beaumont, M. (2008). Joint determination of topology, divergence time, and immigration in population trees. In S. Matsumura, P. Forster, & C. Renfrew (Eds.), *Simulation, genetics and human prehistory* (pp. 135–154). Cambridge: McDonald Institute for Archeological Research.

Beaumont, M. A., Zhang, W., & Balding, D. J. (2002). Approximate Bayesian computation in population genetics. *Genetics*, *162*, 2025–2035.

Bryant, D., & Moulton, V. (2004). Neighbor-net: An agglomerative method for the construction of phylogenetic networks. *Molecular Biology and Evolution*, *21*, 255–265.

Csilléry, K., François, O., & Blum, M. G. B. (2012). abc: An R package for approximate Bayesian computation (ABC). *Methods in Ecology and Evolution*, *3*, 475–479.

Drummond, A. J., & Rambaut, A. (2007). BEAST: Bayesian evolutionary analysis by sampling trees. *BMC Evolutionary Biology*, *7*, 214.

Eidesen, P. B., Carlsen, T., Molau, U., & Brochmann, C. (2007). Repeatedly out of Beringia: *Cassiope tetragona* embraces the Arctic. *Journal of Biogeography*, *34*, 1559–1574.

Eidesen, P. B., Ehrich, D., Bakkestuen, V., Alsos, I. G., Gilg, O., Taberlet, P., & Brochmann, C. (2013). Genetic roadmap of the Arctic: Plant dispersal highways, traffic barriers and capitals of diversity. *New Phytologist*, *200*, 898–910.

Elven, R., Murray, D., Yu, V., & Yurtsev, B. (2007). *Annotated checklist of the Panarctic Flora (PAF) Vascular Plants version*. Retrieved from http://nhm2.uio.no/paf

Evanno, G., Regnaut, S., & Goudet, J. (2005). Detecting the number of clusters of individuals using the software STRUCTURE: A simulation study. *Molecular Ecology*, *14*, 2611–2620.

Excoffier, L., Dupanloup, I., Huerta-Sánchez, E., Sousa, V. C., & Foll, M. (2013). Robust demographic inference from genomic and SNP data. *PLoS Genetics*, *9*, e1003905.

Excoffier, L., & Foll, M. (2011). fastsimcoal: A continuous-time coalescent simulator of genomic diversity under arbitrarily complex evolutionary scenarios. *Bioinformatics*, *27*, 1332–1334.

Falush, D., Stephens, M., & Pritchard, J. K. (2003). Inference of population structure using multilocus genotype data: Linked loci and correlated allele frequencies. *Genetics*, *164*, 1567–1587.

Flot, J. F. (2010). SEQPHASE: A web tool for interconverting phase input/output files and fasta sequence alignments. *Molecular Ecology Resources*, *10*, 162–166.

Frenzel, B., Beug, H., Brunnacker, K., Busche, D., Frankenberg, P., & Geyh, M. A. (1992). Vegetation during the maximum cooling of the last glaciation. In B. Frenzel, M. Pécsi & A. A. Velichko (Eds.), *Atlas of Paleoclimates and Paleoenvironments of the Northern Hemisphere: late Pleistocene-Holocene* (p. 122). Budapest: Geographical Research Institute.

Gibbard, P., & Van Kolfschoten, T. (2004). The Pleistocene and Holocene epochs. In F. M. Gradstein, J. G. Ogg, & A. G. Smith (Eds.), *A geologic time scale* (pp. 441–452). Cambridge: Cambridge University Press.

Gillespie, E. L., & Kron, K. A. (2013). Molecular phylogenetic relationships and morphological evolution within the tribe Phyllodoceae (Ericoideae, Ericaceae). *Systematic Botany*, 38, 752–763.

Gussarova, G., Allen, G. A., Mikhaylova, Y., McCormick, L. J., Mirre, V., Marr, K. L., … Brochmann, C. (2015). Vicariance, long-distance dispersal, and regional extinction-recolonization dynamics explain the disjunct circumpolar distribution of the arctic-alpine plant *Silene acaulis*. *American Journal of Botany*, 102, 1703–1720.

Hata, D., Higashi, H., Yakubov, V., Barkalov, V., Ikeda, H., & Setoguchi, H. (2017). Phylogeographical insight into the Aleutian flora inferred from the historical range shifts of the alpine shrub *Therorhodion camtschaticum* (Pall.) Small (Ericaceae). *Journal of Biogeography*, 44, 283–293.

Heled, J., & Drummond, A. J. (2010). Bayesian inference of species trees from multilocus data. *Molecular Biology and Evolution*, 27, 570–580.

Hewitt, G. M. (1996). Some genetic consequences of ice ages, and their role in divergence and speciation. *Biological Journal of the Linnean Society*, 58, 247–276.

Hey, J. (2010). Isolation with migration models for more than two populations. *Molecular Biology and Evolution*, 27, 905–920.

Hey, J., & Nielsen, R. (2007). Integration within the Felsenstein equation for improved Markov chain Monte Carlo methods in population genetics. *Proceedings of the National Academy of Sciences of the United States of America*, 104, 2785–2790.

Hultén, E. (1937). *Outline of the history of arctic and boreal biota during the quarternary period*. Stockholm: Bokförlags aktiebolaget Thule.

Ikeda, H. (2012). Genetic diversity in multilocus nuclear genes of *Phyllodoce nipponica* (Ericaceae). *Bulletin National Museum of Nature and Science Series B*, 34, 55–61.

Ikeda, H., Fujii, N., & Setoguchi, H. (2009). Application of the isolation with migration model demonstrates the pleistocene origin of geographic differentiation in *Cardamine nipponica* (Brassicaceae), an endemic Japanese alpine plant. *Molecular Biology and Evolution*, 26, 2207–2216.

Ikeda, H., Higashi, H., Yakubov, V., Barkalov, V., & Setoguchi, H. (2014). Phylogeographical study of the alpine plant *Cassiope lycopodioides* (Ericaceae) suggests a range connection between the Japanese archipelago and Beringia during the Pleistocene. *Biological Journal of the Linnean Society*, 113, 497–509.

Ikeda, H., Sakaguchi, S., Yakubov, V., Barkalov, V., & Setoguchi, H. (2016). Importance of demographic history for phylogeographic inference on the arctic-alpine plant *Phyllodoce caerulea* in East Asia. *Heredity*, 116, 232–238.

Ikeda, H., Senni, K., Fujii, N., & Setoguchi, H. (2006). Refugia of *Potentilla matsumurae* (Rosaceae) located at high mountains in the Japanese archipelago. *Molecular Ecology*, 15, 3731–3740.

Ikeda, H., Senni, K., Fujii, N., & Setoguchi, H. (2008). Consistent geographic structure among multiple nuclear sequences and cpDNA polymorphisms of *Cardamine nipponica* Franch. et Savat. (Brassicaceae). *Molecular Ecology*, 17, 3178–3188.

Ikeda, H., Senni, K., Fujii, N., & Setoguchi, H. (2009). High mountains of the Japanese archipelago as refugia for arctic-alpine plants: Phylogeography of *Loiseleuria procumbens* (L.) Desvaux (Ericaceae). *Biological Journal of the Linnean Society*, 97, 403–412.

Ikeda, H., & Setoguchi, H. (2010). Natural selection on *PHYE* by latitude in the Japanese archipelago: Insight from locus specific phylogeographic structure in *Arcterica nana* (Ericaceae). *Molecular Ecology*, 19, 2779–2791.

Ikeda, H., & Setoguchi, H. (2013). A multilocus sequencing approach reveals the cryptic phylogeographical history of *Phyllodoce nipponica* Makino (Ericaceae). *Biological Journal of the Linnean Society*, 110, 214–226.

Ikeda, H., Yakubov, V., Barkalov, V., & Setoguchi, H. (2014). Molecular evidence for ancient relicts of arctic-alpine plants in East Asia. *New Phytologist*, 203, 980–988.

Ikeda, H., Yoneta, Y., Higashi, H., Eidesen, P. B., Barkalov, V., Yakubov, V., … Setoguchi, H. (2015). Persistent history of the bird-dispersed arctic-alpine plant *Vaccinium vitis-idaea* L. (Ericaceae) in Japan. *Journal of Plant Research*, 128, 437–444.

Jakobsson, M., & Rosenberg, N. A. (2007). CLUMPP: A cluster matching and permutation program for dealing with label switching and multimodality in analysis of population structure. *Bioinformatics*, 23, 1801–1806.

Liu, S., Denford, K. E., Ebinger, J. E., Packer, J. G., & Tucker, G. C. (1993). Kalmia. In Flora of North America Editorial Committee E (Ed.), *Flora of North America North of Mexico* 20+vols. (pp. 480–485). New York, NY and Oxford: Oxford University Press.

Massatti, R., & Knowles, L. L. (2016). Contrasting support for alternative models of genomic variation based on microhabitat preference: Species-specific effects of climate change in alpine sedges. *Molecular Ecology*, 25, 3974–3986.

Murray, D. (1995). Causes of arctic plant diversity: Origin and evolution. In S. Chapin, & C. Korner (Eds.), *Arctic and alpine biodiversity: Patterns, causes and ecosystem consequences* (pp. 21–32). Heidelberg: Springer.

Nielsen, R., & Beaumont, M. A. (2009). Statistical inferences in phylogeography. *Molecular Ecology*, 18, 1034–1047.

Ossowski, S., Schneeberger, K., Lucas-Lledó, J. I., Warthmann, N., Clark, R. M., Shaw, R. G., … Lynch, M. (2010). The rate and molecular spectrum of spontaneous mutations in *Arabidopsis thaliana*. *Science*, 327, 92–94.

Popp, M., Mirre, V., & Brochmann, C. (2011). A single Mid-Pleistocene long-distance dispersal by a bird can explain the extreme bipolar disjunction in crowberries (*Empetrum*). *Proceedings of the National Academy of Sciences of the United States of America*, 108, 6520–6525.

Pritchard, J. K., Stephens, M., & Donnelly, P. (2000). Inference of population structure using multilocus genotype data. *Genetics*, 155, 945–959.

Shimizu, T. (1982). *The new alpine flora of Japan in color Vol. I*. Osaka, Japan: Hoikusha Publishing.

Sim, Z., Hall, J. C., Jex, B., Hegel, T. M., & Coltman, D. W. (2016). Genome-wide set of SNPs reveals evidence for two glacial refugia and admixture from postglacial recolonization in an alpine ungulate. *Molecular Ecology*, 25, 3696–3705.

Stephens, M., & Donnelly, P. (2003). A comparison of Bayesian methods for haplotype reconstruction from population genotype data. *American Journal of Human Genetics*, 73, 1162–1169.

Stephens, M., Smith, N. J., & Donnelly, P. (2001). A new statistical method for haplotype reconstruction from population data. *American Journal of Human Genetics*, 68, 978–989.

Sun, Y., Surget-Groba, Y., & Gao, S. (2016). Divergence maintained by climatic selection despite recurrent gene flow: A case study of *Castanopsis carlesii* (Fagaceae). *Molecular Ecology*, 25, 4580–4592.

Tajima, F. (1983). Evolutionary relationship of DNA sequences in finite populations. *Genetics*, 105, 437–460.

Tajima, F. (1989). Statistical method for testing the neutral mutation hypothesis by DNA polymorphism. *Genetics*, 123, 585–595.

Wang, Q., Liu, J., Allen, G. A., Ma, Y., Yue, W., Marr, K. L., & Abbott, R. J. (2016). Arctic plant origins and early formation of circumarctic distributions: A case study of the mountain sorrel, *Oxyria digyna*. *New Phytologist*, 209, 343–353.

Wei, H., Fu, Y., & Arora, R. (2005). Intron-flanking EST-PCR markers: From genetic marker development to gene structure analysis in *Rhododendron*. *Theoretical and Applied Genetics*, 111, 1347–1356.

Westergaard, K. B., Jørgensen, M. H., Gabrielsen, T. M., Alsos, I. G., & Brochmann, C. (2010). The extreme Beringian/Atlantic disjunction in *Saxifraga rivularis* (Saxifragaceae) has formed at least twice. *Journal of Biogeography*, 37, 1262–1276.

Wolfe, K. H., Li, W. H., & Sharp, P. M. (1987). Rates of nucleotide substitution vary greatly among plant mitochondrial, chloroplast, and nuclear DNAs. *Proceedings of the National Academy of Sciences of the United States of America*, 84, 9054–9058.

Yamazaki, T. (1993). Ericaceae 4. *Loiseleuria*. In K. Iwatsuki, T. Yamazaki, D. E. Goufford, & H. Ohba (Eds.), *Flora of Japan IIIa* (pp. 8–9). Tokyo: Kodansha.

SUPPORTING INFORMATION

Additional Supporting Information may be found online in the supporting information tab for this article.